JOURNAL OF MATERIALS SCIENCE 16 (1981) 331–340

Relationships between mechanical behaviour and craze morphology in thin films of polystyrene

J. S. TRENT
Department of Mechanics and Materials Science, Rutgers, The State University of New Jersey, P.O. Box 909 Piscataway, New Jersey 08854, USA

I. PALLEY, E. BAER
Department of Macromolecular Science, Case Western Reserve University, Cleveland, Ohio 44106, USA

A new technique has been developed to study the relationship between mechanical properties and craze microstructure in thin films (1 to 5 μm) of polystyrene. Thin film samples of thicknesses in this range could be strained in a conventional testing machine and subsequently examined in the deformed state in an electron microscope. The strain rate was systematically varied and its effect was investigated on both quenched and annealed samples. Correlations were found between craze morphology and ductility. A new "craze parameter" has been defined as the width of a strip of material which is involved in the development of a craze. From this value, the average strain and the average volume fraction of fibrils within a craze can be calculated.

1. Introduction

The degree of brittleness in glassy polymers is mainly determined by the generation of crazes propagating perpendicularly to an applied stress [1, 2]. It is also accepted that crazes develop in regions of localized inhomogeneities within the material or at stress-raising flaws. However, a study of the literature indicates that there is no agreement among authors beyond these elementary points.

Gent [3] proposed that the dilatant stress component at the tip of a flaw can be high enough to transform glassy material into the rubbery state. The devitrified polymer cavitates under negative pressure and forms a craze. Sternstein and Ongchin [4] and Rusch and Beck [5, 6] proposed that the dilatational stress field increases molecular mobility by increasing the free volume. Haward [7] and Andrews and Bevan [8] argue that the controlling parameter for craze formation is the hydrostatic cavitational stress for void growth. While Haward [7] and Argon [9] proposed that voids nucleate in clusters rather than singly ahead of the craze tip. At some critical value of porosity the voids become interconnected. They suggested that because of the interconnections the hydrostatic cavitational stress is lower than the yield stress. In support of this view, Wellinghoff and Baer [10] showed that the surface microstructure of thin films was sufficiently heterogeneous to initiate localized strain inhomogeneities of approximately 300 Å in diameter. These localized zones ultimately coalesced along the minor principal stress direction. The formation of narrow disk-shaped plastic zones propagating perpendicular to the applied strain was described. Olf and Peterlin [11] modified Gent's proposal by stating that the negative pressure at a flaw reduces only the yield stress of the polymer at that point.

Though these authors [3–11] disagree on how crazes initiate, they all agree that crazes ultimately form by cavitation under some hydrostatic stress produced within the polymer at various stress raising flaws. Little is known about the distribution of stresses and strains within a single craze. This lack of knowledge complicates any attempts

0022–2461/81/020331–10$03.00/0

to explain mechanisms of craze formation. Since craze formation is based largely on void formation and free volume criteria, it was surprising to find that no study has been conducted relating craze morphology to variations in thermal history. By varying the "free volume" content, a better understanding is gained of the proposed mechanisms for craze formation. A technique to study the relationship between the mechanical properties and craze microstructure in thin films of polystyrene has been developed. In addition, a systematic investigation showing the effect of thermal history on polystyrene has been carried out.

Wellinghoff and Baer [10], Beahan, Bevis and Hull [12], and Kramer [13], have studied the initiation and growth of crazes by examining strained PS thin films having thicknesses of 500 to 7500 Å using transmission electron microscopy (TEM). Polystyrene (PS) films used in this study are between 2.3 and 2.7 μm thick. Many advantages are realized when this increased thickness is employed. Specimens cut from these films are sufficiently strong to support themselves without substrate and this fact enables their stress–strain behaviour to be readily recorded. Crazes can grow freely through the film and are influenced only by other crazes, impurities or defects within the PS matrix. Previous studies of craze microstructure involved microtoming strained bulk specimens to obtain crazed samples thin enough for TEM. However, microtoming can cause craze fibril distortion. Although the films used in this study are near the upper limit of thickness for use in the electron microscope, they can be examined directly and produce high resolution micrographs.

Mechanisms explaining craze growth have received insufficient attention. There is no agreement on the mechanisms by which a craze thickens as it increases in length. Two possible thickening mechanisms for craze growth have been proposed. Verhyelpen-Heymans and Bauwens [14] have suggested that the thickening of the craze is due to creep of craze material. They postulate that no material is drawn into the craze during its growth. This mechanism has been termed fibril creep by Kramer [13]. Kramer argues that this mechanism is not dominant in the thickening of crazes. He believes that crazes thicken mainly by drawing new polymer from the polymer matrix into the craze. Beahan, Bevis and Hull [12] suggest that, at low strain-rates, crazes increase in thickness by the drawing of further matrix material into the craze and to some extent by an increase in the orientation of the fibrils.

To investigate the proposed mechanisms, the width of material in the unstressed film that finally is involved in the formation of the craze must be measured. By using the thin-film technique described in this paper, it has been possible to determine this width. Also, it was possible to calculate values of the average strain and volume fraction of fibrils within a single craze.

2. Experimental procedure

2.1. Film preparation and deformation

Solvent-cast thin films of general purpose atactic polystyrene (PS), generously supplied by Dow Chemical Company, were prepared as follows. A 13 wt % solution of PS in O-xylene was prepared. Thin films (2.0 to 2.7 μm thick) were cast by dipping clean glass slides into the solution and then evaporating the solvent. The evaporation was performed by immediately placing the coated glass slides in a vacuum oven for 1 h at room temperature and subsequently raising the temperature slowly to 70° C. Solvent removal was continued at this temperature for an additional 12 h.

Before the thin-film was removed from the glass slide, it was cut with a razor-blade into the shape illustrated in Fig. 1a using a metal template as a guide. This design was chosen to avoid premature failure in the grips. The residual stress left along the edges of the tensile specimen (after cutting) was relieved by annealing on the glass slide for 12 h at 105° C under vacuum. No trace of O-xylene could be detected in the film using Fourier-Transform Infra-red (FTIR) spectroscopy for detection after this final step.

To study the effect of thermal history on the mechanical properties and craze microstructure, samples were either slowly cooled to room temperature at a rate of $13^\circ\,C\,h^{-1}$ (annealed) or quenched in an ice water-bath (quenched) both from 105° C. After such thermal treatment, the specimens were removed from the glass slides by flotation on the surface of a water bath, and subsequent drying on filter paper.

The PS specimens were strained in tension using a conventional Instron testing machine. A sensitive load cell was used which gave a full-scale range of 20 g. Due to accuracy limitations inherent in this type of experiment, meaningful modulus data could not be obtained. For this reason, only the craze initiation stress, the upper

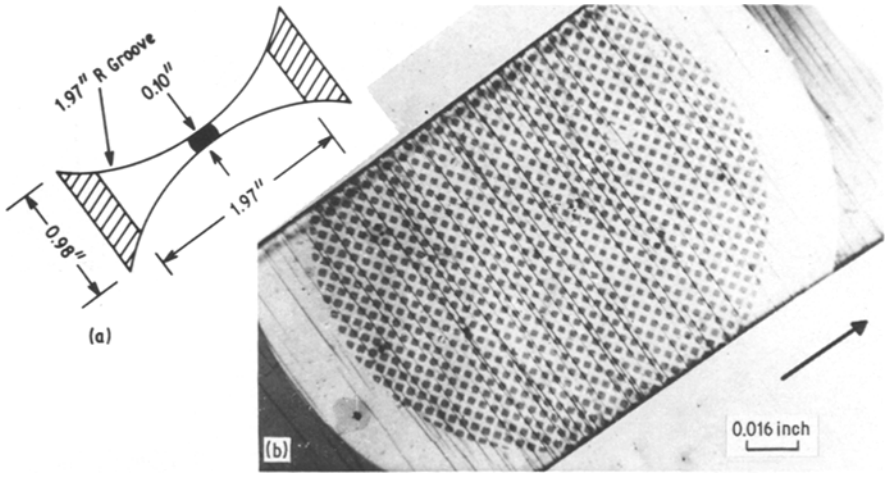

Figure 1 (a) Geometry of thin film polystyrene specimen; all are in inches. (b) Optical photograph of a gold shadowed grid on the surface of a specimen. The arrow indicates direction of applied stress. $\epsilon = 0.76\,\%$; $\dot{\epsilon} = 0.02$ inches min^{-1}; $t = 2.4\,\mu\text{m}$.

yield stress, the fracture stress and the ultimate elongation are reported. The strain rates were 0.002, 0.008, 0.02 and 0.2 inches min^{-1} for the annealed specimens, and were 0.02, 0.10, 0.20 and 0.5 inches min^{-1} for the quenched specimens. Accurate thickness determinations were made by following the method described by Tolansky [15] using FTIR.

2.2. Preparation of specimens for transmission electron microscopy

Specimens for viewing in the transmission electron microscope (TEM) were strained to approximately 0.8% and removed from the Instron in the stressed state. This was done by quickly sandwiching the sample between two glass plates, one of which contained two strips of double-sided sticky tape. Ultimately, stress relaxation did occur, but this technique kept the fine craze microstructure from re-orienting. To insure dimensional stability for viewing in the electron microscope, a thin coating of platinum metal and carbon was shadowed onto the surface. The platinum metal gave a good contrast for examination of the craze microstructure. With an optical microscope, selected areas of the stressed specimens were cut and placed between 100 mesh folding copper grids, and subsequently observed in a Hatachi HU-11A electron microscope.

2.3. Thickness determination of material in the craze

The width of a strip of material finally involved in a craze, W_0, was determined by evaporating gold onto the surface through a 400 mesh copper grid. Then these specimens were strained (Fig. 1b), and lightly coated with carbon. Carbon improves contrast and also conducts away some of the heat produced by the electron beam.

To understand the experimental technique for the determination of W_0, consider first the schematic drawings in Figs 2 and 3 which show the results of both a crack and craze which have propagated through the tilt edge of a shadowed zone. Fig. 2a represents the condition before stress is applied. The dashed line indicates the direction of a line along which a crack will propagate, and the shadowed zone is tilted ϕ degrees to the direction of crack propagation. When stress is applied (Fig. 2b), the shadowed zone is separated due to the propagation of the crack by a distance equal to the crack width, W_f. Since a crack contains no material, $W_0 = 0$. All points along the line of propagation will separate in a vertical fashion with respect to each other a distance of W_f, as illustrated in Fig. 2a and b.

A craze, unlike a crack, contains material; so one must consider how this shadowed zone will separate with craze propagation. Fig. 3a shows the condition before stress is applied. It will be assumed that all the material between the dashed lines will ultimately make up the observed craze and also the material outside the dashed lines will not be involved in craze formation. Therefore, W_0 is defined as the width between the dashed lines. The shadowed zone is tilted at angle ϕ to the

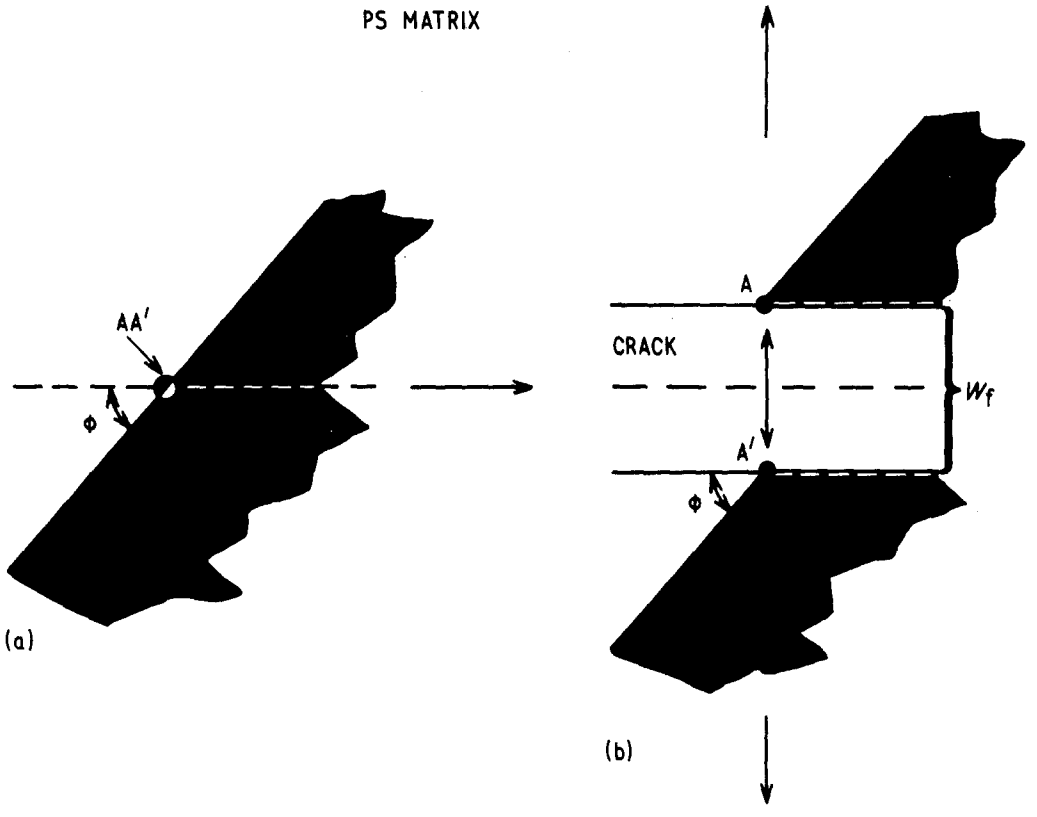

Figure 2 A scheme of crack propagation through tilt edge of a shadowed zone; (a) before stress is applied, (b) after stress is applied. The large arrows indicate direction of applied stress.

boundary of the bottom dashed line. By measuring Δ, the horizontal length between points A and A^1, W_0 can be determined by

$$W_0 = \Delta \tan \phi. \quad (1)$$

Once stress is applied (Fig. 3b), the shadowed zone will deform, but not as if a crack had propagated through it. The shadowed area between the dashed lines will become less dense due to deformation of involved material. One can see that Δ never changes as long as the material between the dashed lines elongates. If a measure of ϕ, Δ and W_f (final craze width) is made after deformation, then the average strain within the craze ($\bar{\epsilon}_c$) and the average volume fraction of craze fibrils ($\bar{V}_f$) can be calculated by

$$\bar{\epsilon}_c = \ln \frac{W_f}{W_0} \quad (2)$$

and

$$V_f = \frac{W_0}{W_f}. \quad (3)$$

This experiment was performed on both annealed and quenched samples.

3. Results

3.1. Effect of thermal history and strain rate on stress–strain behaviour

Fig. 4a shows the stress–strain behaviour at various strain rates for the annealed thin films of PS tested in tension. The curves in Fig. 4a and b are an average of at least three runs. At strain rates of 0.002, 0.008 and 0.02 inches min^{-1}, the thin films exhibited ductile behaviour and showed distinct yield points. As the strain rate increased, the elongation to break decreased while the craze initiation stress, yield stress and fracture stress increased. Craze initiation occurs at the stress which corresponds to the onset of non-linearity on the stress–strain curve. At a strain rate of 0.2 inches min^{-1} the films fractured in a brittle manner.

Fig. 4b shows the stress–strain curves with various strain rates for thin film specimens rapidly

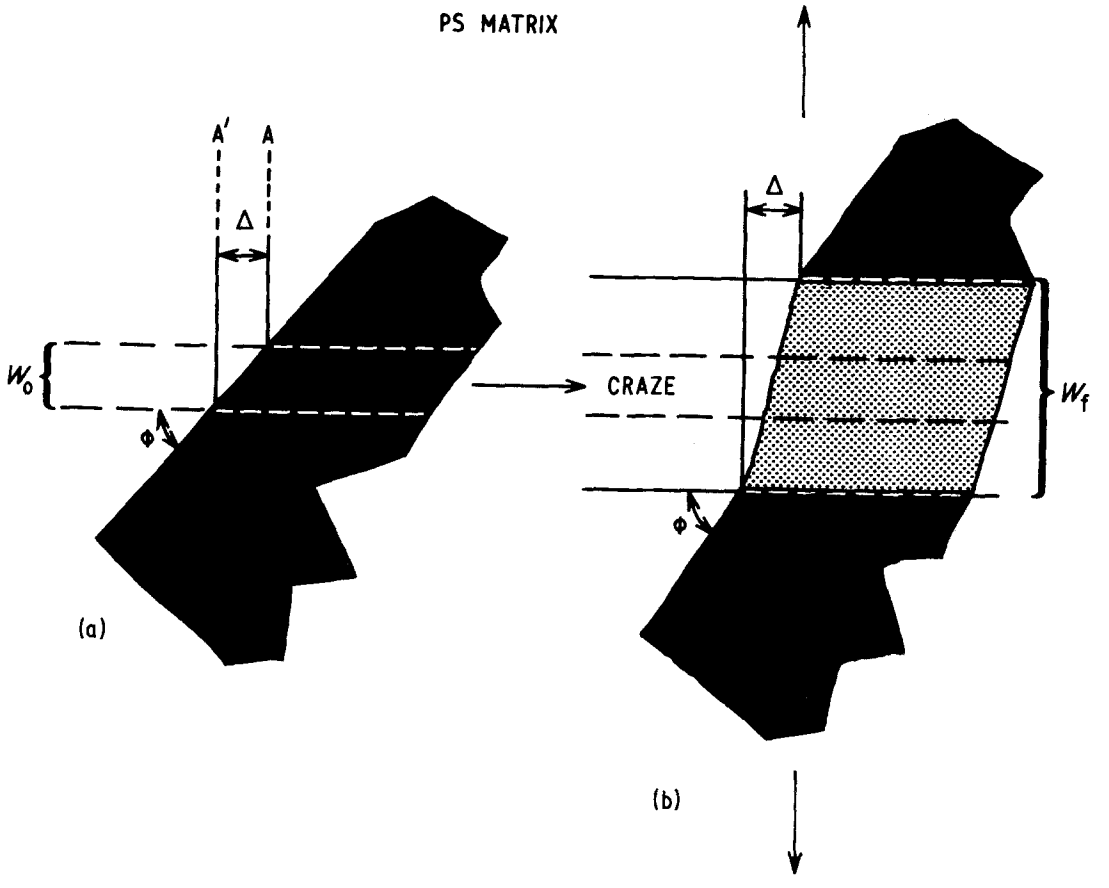

Figure 3 A scheme of craze propagation through tilt edge of a shadowed zone; (a) before stress is applied, (b) after stress is applied. The large arrows indicate direction of applied stress.

quenched from their annealing temperatures. At strain rates of 0.02, 0.10 and 0.20 inches min^{-1}, these films exhibited ductile behaviour and showed distinct yield points. As in Fig. 4a the elongation to break decreased and the craze initiation stress, yield stress and fracture stress increased with increasing strain rate. At a strain rate of 0.5 inches min^{-1} the films exhibited brittle fracture.

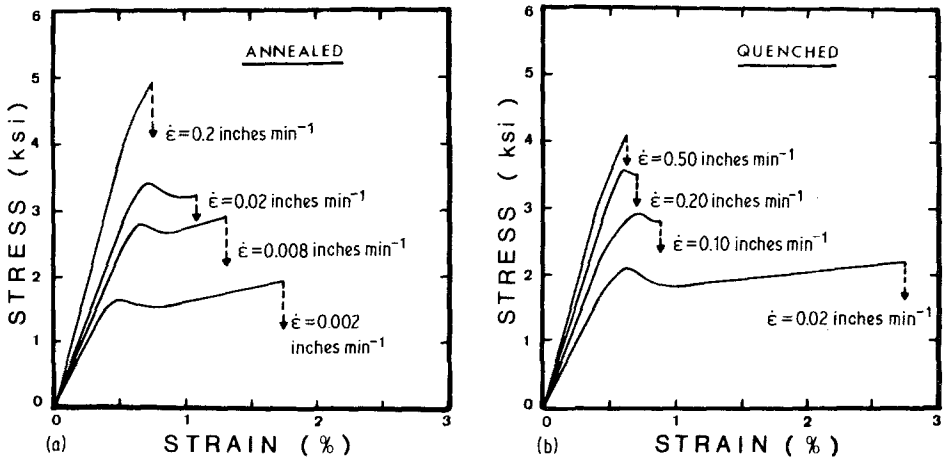

Figure 4 Stress–strain curves as a function of strain rate for (a) annealed and (b) quenched thin-film PS specimens in tension. All strain rates are given in inches min^{-1}.

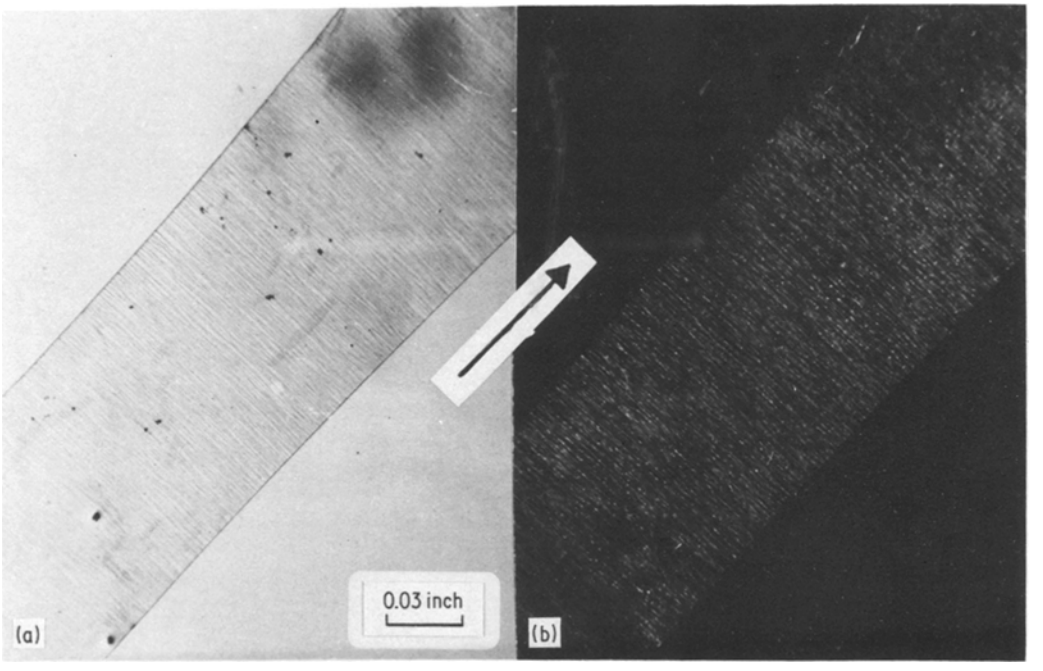

Figure 5 Optical photographs of gauge area for quenched thin-film PS specimen with: (a) parallel polarizers, (b) crossed polarizers. Arrow indicates direction of applied stress. $\epsilon = 2.8\,\%$; $\dot{\epsilon} = 0.02$ inches min^{-1}; $t = 2.7\,\mu\text{m}$.

Ductility for both annealed and quenched material was attributed mainly to the formation of crazes which grow perpendicularly to the direction of applied stress. This can be clearly seen in Fig. 5, which is an optical micrograph showing the gauge area of a quenched thin film strained at $\dot{\epsilon} = 0.02$ inches min^{-1}. Fig. 5a was taken with the polarizers parallel to each other, and Fig. 5b shows the craze film between crossed polarizers. The arrow indicates the direction of applied stress. Crazing seems to be the only deformation mechanism and is responsible for the observed ductility seen in Fig. 4a and b. Nielson [16] has given a description of how crazes can be responsible for large elongations in polymers. It is apparent that the yield stress, fracture stress and craze initiation stress for the annealed specimens were considerably higher than those of the quenched specimens deformed under equal strain rates. However, at a given strain rate, the elongation to break was much larger for the quenched thin films than for those which were annealed. At $\dot{\epsilon} = 0.02$ inches min^{-1}, the quenched specimens had a maximum elongation of approximately 2.8 % while that of the annealed specimens was approximately 1.2 %. A ten-fold increase in the strain rate for the annealed material produced brittle behaviour. In contrast, the quenched films remained ductile, although a ten-fold increase in strain rate greatly reduced the elongation to break.

Based on these results, it appears that by increasing strain rate or by annealing, the tendency toward brittle behaviour is increased. However, these results alone cannot explain why the quenched material is more ductile than the annealed material. A detailed look at craze morphology as related to the observed mechanical properties for both annealed and quenched samples provided a deeper insight into this problem.

3.2. Effect of thermal history and strain rate on craze morphology

An electron micrograph of a typical craze formed in an annealed sample is shown in Fig. 6a. This particular sample was strained at $\dot{\epsilon} = 0.02$ inches min^{-1} and drawn to break. The craze shown was in the "mature" region several hundred microns from the craze-tip. The width of such crazes averaged approximately 2 μm. A common characteristic of many crazes was a pronounced "void" region near the centre of the craze having an average width of about 2000 Å. The polymer within this void region appears to be a three-dimensional array of interconnected fibrils with

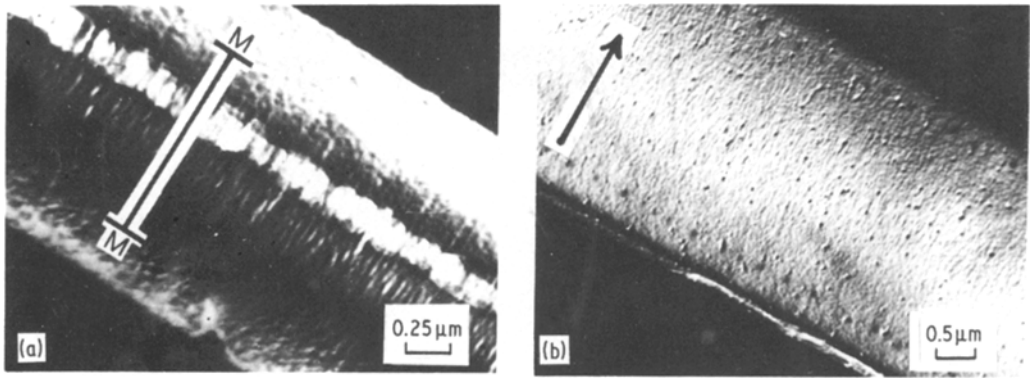

Figure 6 Electron micrographs of a typical craze, formed in (a) annealed and (b) quenched specimens at $\dot{\epsilon} = 0.02$ inches min^{-1}. The micrographs were taken after fracture. The arrow indicates direction of applied stress and distance M–M defines the thickness of the mid-rib.

diameters ranging between 200 and 500 Å. This type of voiding was observed by Beahan *et al.* [17] in crazes formed in thin films that were similarly prepared. Fine fibrils 200 to 400 Å wide can be observed on either side of this void region. However, this fine structure does not traverse the entire width of the craze. Beahan *et al.* [17] have defined this void area as the mid-rib section of the craze. We will define the mid-rib region as the width of the observable fine fibrillar structure plus the width of the void region, if present. This definition was adopted because all crazes contained a region of fine fibrillar structure, but did not necessarily contain a void region. It is possible that in annealed materials voiding of the mid-rib area occurs just before fracture.

Fig. 6b shows an electron micrograph of a typical craze formed in films quenched into ice water from a temperature of 105° C. This sample was strained at $\dot{\epsilon} = 0.02$ inches min^{-1} and drawn to break. Again, this micrograph was obtained from a region several hundred microns from the craze-tip. The widths of these crazes ranged from 3.4 to 4.0 μm. As was observed for the annealed case, fine fibrils normal to the craze boundaries nearly spanned the entire width of the craze. This fibril-type structure had a uniform width averaging 350 Å, and had no noticeable void region between fibrils. The fibrils were more distinguishable along the centre of the craze and became less pronounced near the craze–matrix interface.

3.3. Craze morphology and ductility

Examination of the stress–strain curves in Fig. 4 reveals that samples quenched in ice water elongated 2.5 times more than the samples slowly cooled to room temperature. This effect is reflected in the final craze widths. The "quenched" crazes were approximately 2 times wider than the "annealed" crazes. However, the fibrils within the mid-rib region for both types of crazes were similar in width and appearance. The most pronounced difference was the appearance of a void region within the mid-rib section of the "annealed" crazes. This void region was not seen in the quenched films strained at $\dot{\epsilon} = 0.02$ inches min^{-1}. The mid-rib width of "quenched" crazes was approximately 2.5 times larger than that of the "annealed" crazes. Quenching the thin films seems to have decreased the propensity for void growth in the mid-rib region and increased the uniformity of deformation.

A series of electron micrographs of crazes formed in films quenched from 105° C are shown in Fig. 7. These micrographs are from the mature region several hundred microns from the craze-tip. Each sample was strained to similar strains of 0.8 %. Fig. 7a, b and c were strained at $\dot{\epsilon} = 0.002$, 0.02 and 0.2 inches min^{-1}, respectively. It appears that an increase in strain rate produces a decrease in both W_f (final craze width) and the mid-rib width. However, a fine fibrillar structure is still observed in the mid-rib region. A clearer understanding of how mid-rib region changes with strain rate can be gained from a plot of (mid-rib width/W_f) against strain rate (Fig. 8).

Fig. 8 shows that the width of the mid-rib decreases linearly with increasing strain rate. It appears that high strain rates localized deformation near the centre of the craze. Also, craze density was found to increase with increasing strain rate. Stress–strain curves for quenched

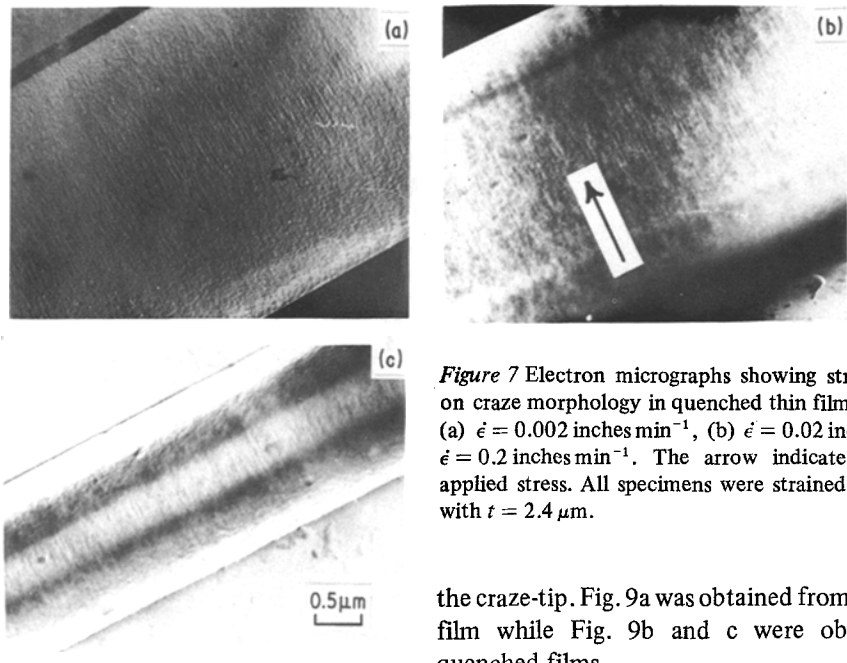

Figure 7 Electron micrographs showing strain rate effect on craze morphology in quenched thin film PS specimens; (a) $\dot{\epsilon} = 0.002$ inches min^{-1}, (b) $\dot{\epsilon} = 0.02$ inches min^{-1}, (c) $\dot{\epsilon} = 0.2$ inches min^{-1}. The arrow indicates direction of applied stress. All specimens were strained to $\epsilon = 0.76\%$, with $t = 2.4\,\mu$m.

samples at $\dot{\epsilon} = 0.2$ inches min^{-1} resembled those of annealed samples at $\dot{\epsilon} = 0.02$ inches min^{-1} (Fig. 4). It has been found that the morphology of crazes for quenched material at a high strain rate is similar to the morphology of the crazes for annealed material for a low strain rate. Therefore the mechanical behaviour is determined by craze morphology.

After straining to 0.8%, samples with gold mesh were examined in the electron microscope. Fig. 9a and b shows electron micrographs in the mature region several hundred microns from the craze-tip of a single craze that was propagated through the tilt edge of a gold shadowed region. Fig. 9c shows a region approximately 40 μm from the craze-tip. Fig. 9a was obtained from an annealed film while Fig. 9b and c were obtained from quenched films.

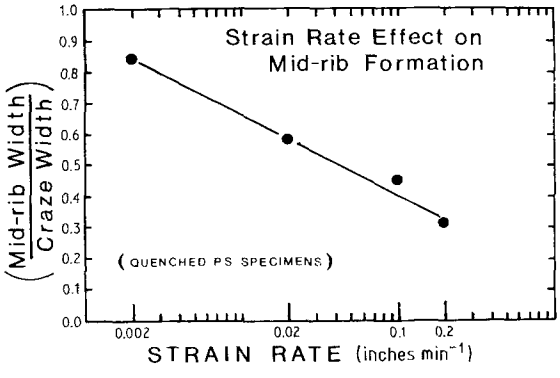

Figure 8 Plot of (mid-rib width/craze width) against strain rate showing effect of strain rate on mid-rib for quenched PS specimens.

The resemblance of Fig. 9a to Fig. 9b suggests that these crazes developed in a similar manner. It is also interesting to note that the gold particles within both crazes separated from each other in a similar fashion. They appear to form layers parallel to the craze boundary. From measurements of Δ, ϕ and W_f for each craze, W_0, $\bar{\epsilon}_c$ and $\bar{V}_f$ were calculated. The results of these calculations are summarized in Table I for the two specimens differing only in thermal history. Crazes in both quenched and annealed films had approximately equal values of W_0 and W_f. The thermal history did not alter W_0, $\bar{\epsilon}_c$ or $\bar{V}_f$. At equal strain, the stress for the annealed specimens was considerably larger than that for the quenched specimens (Fig. 4). It can be seen that W_0 for Fig. 9b is almost twice as large as that for Fig. 9c. This evidence suggests that as the craze thickens by fibril extension, material is also drawn into the craze from the craze–matrix interface.

4. Discussion

Fig. 4a and b present the thermal history and average strain rate effects on mechanical properties of polystyrene. Annealing of the polymer film produces a more dense intermolecular chain packing than quenching. It appears that plastic deformation, due to a nondestructive process, can be produced more easily in quenched films, other conditions being equal. The relative strain rate experienced in the crazed material can cause

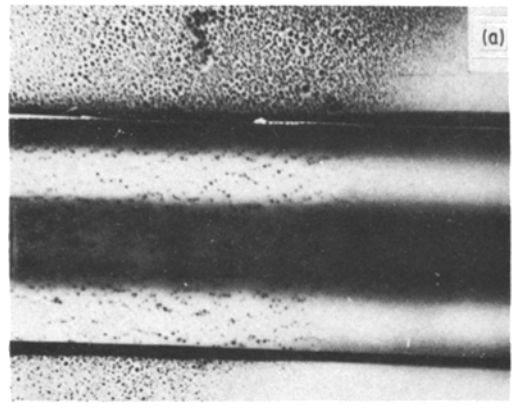

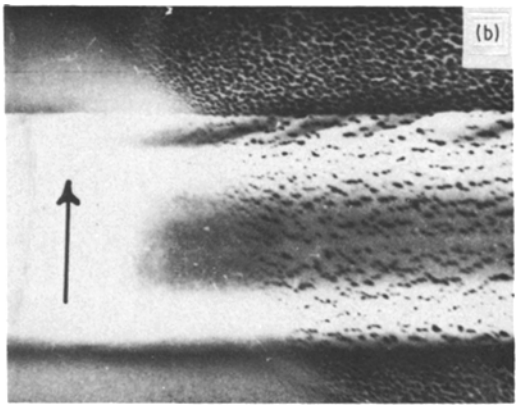

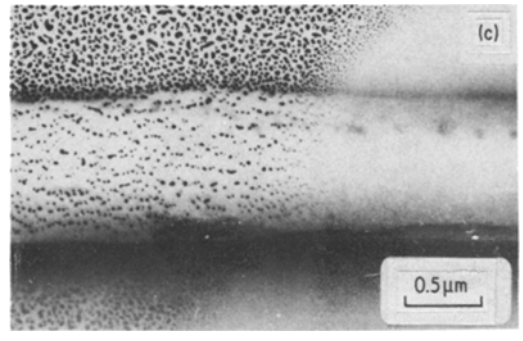

Figure 9 Electron micrographs of a section of a craze propagated through tilt edge of a gold shadowed zone; (a) annealed specimen, (b) quenched specimen, (c) quenched specimen ~ 40 μm near craze-tip. Arrow indicates direction of applied stress. $\epsilon = 0.76\%$; $\dot{\epsilon} = 0.02$ inches min^{-1}; $t = 2.3\,\mu m$.

destructive deformation in annealed films (voided mid-rib) and nondestructive deformation in quenched films (nonvoided mid-rib). A manifestation of this morphological difference is seen between annealed and quenched samples at a strain rate of 0.02 inches min^{-1} (and at various strain rates) (Fig. 4), observing the difference in "ductility". Please note that ductile deformation in all of these thermally treated specimens is largely confined within the crazes. Experiments using thin films provide a sensitive technique for examining deformation processes within crazes. Though the stress–strain curves in Fig. 4 are characteristic of ductile behaviour, elongations are only between 1 and 3%. 3% elongation-to-fracture in bulk specimens is generally considered to be brittle fracture. So, any consideration of ductility in polystyrene thin films is concerned with deformation processes within the craze.

It appears from our experimental results that at some time during the tensile experiment, flow of additional material into the craze must have ceased giving crazes of uniform thickness along its length and equal W_0 for both "annealed" and "quenched" crazes (Table I) far removed from the craze-tip. A straight, sharp boundary between elastically and inelastically deformed material was observed, being typical for mature crazes. We believe that at some moment during the deformation process, the forces exerted by the fibrils on the elastically deformed matrix are at times not enough to involve new material. At this moment, all deformations concentrate inside the craze. Through strain hardening of the fibrils, forces may build up enough to incorporate new material into the craze, resulting in a cyclic stress profile, causing the gold particles in Fig. 9 to separate from each other in layers parallel to the craze boundary. This explains why W_0 in Fig. 9c is less than W_0 in Fig. 9b. With the fact that the volume fraction of craze fibrils, $\bar{V}_f$, and the average strain within the craze, $\bar{\epsilon}_c$, remain constant with increasing craze width, W_f (Table I), these results suggest that W_0 increases (in steps) going away from the

TABLE I Thermal history effect on crazing parameters for quenched thin films of PS

Thermal history	ϕ	Δ (μm)	W_0 (μm)	W_f (μm)	$\bar{\epsilon}_c$	$\bar{V}_f$
Annealed*	47°	0.57	0.61	1.71	1.03	0.36
Quenched*	43°	0.64	0.60	1.68	1.03	0.36
Quenched†	43°	0.39	0.36	1.00	1.02	0.36

*Micrograph in mature region far removed from craze-tip.
†Micrograph ~ 40 μm near craze-tip; $\epsilon = 0.76\%$, $\dot{\epsilon} = 0.02$ inches min^{-1}, $t = 2.3\,\mu m$, $\phi \pm 2°$, $\Delta \pm 0.03\,\mu m$, $W_0 \pm 0.08\,\mu m$, $W_f \pm 0.03\,\mu m$.

craze tip, meaning that material is drawn into the craze from the craze–matrix interface. More experiments remain to be conducted in order to verify this point.

5. Conclusions

The macro-mechanical properties of thin films of polystyrene are strongly affected by thermal history. The yield level is higher for annealed than for quenched films, all other conditions being equal. Both annealed and quenched films become more ductile with decreasing average strain rate. At the micro-level, thermal history affects the response of a microvolume of material to local strain rates, which also affects craze morphology and the localized mechanical resistance.

Studies using high resolution electron microscopy showed the relationships between craze morphology and the observed ductility. Brittle behaviour is always observed in samples with voiding mid-ribs in the craze. As a craze thickens by fibril extension, material is simultaneously drawn into the craze from the craze–matrix interface. Strips of material are drawn into the craze until at some critical point drawing stops and the craze thickens only by fibril extension.

Acknowledgements

The principal author thanks the Lord his God for the accomplishment of this work. The authors wish to thank the Office of Naval Research for its generous financial support. We would also like to thank Dr Rowan Truss and Dr Stephen Wellinghoff for their stimulating discussions and helpful suggestions.

References

1. S. RABINOWITZ and BEARDMORE, "CRC Critical Reviews in Macromolecular Science", Vol. 1, edited by E. Baer, P. Geil and J. Koenig CRC Press, Cleveland, 1972) p. 1.
2. R. P. KAMBOUR, *J. Polymer Sci. Macromol. Rev.* 7 (1973) 1.
3. A. N. GENT, *J. Mater. Sci.* 5 (1970) 925.
4. S. S. STERNSTEIN and L. ONGCHIN, *Polymer Prep.* **10** (1969) 117.
5. K. C. RUSCH and R. H. BECK, Jr, *J. Macromol. Sci-Phys.* **B3** (1969) 365.
6. *Idem, ibid.* **B4** (1970) 261.
7. R. N. HAWARD, in "Amorphous Materials", edited by R. W. Douglas and B. Ellis (Wiley Interscience, London and New York, 1972) p. 513.
8. E. H. ANDREWS and L. BEVAN, *Polymer* **13** (1972) 337.
9. A. S. ARGON, *J. Macromol. Sci. Phys.* **B8** (1963) 573.
10. S. WELLINGHOFF and E. BAER, *ibid.* **B11** (1975) 367.
11. H. G. OLF and A. PETERLIN, *J. Polymer Sci. A-2* **12** (1974) 2209.
12. P. BEAHAN, M. BEVIS and D. HULL, *J. Mater. Sci.* **B7** (1972) 162.
13. E. J. KRAMER, in "Developments in Polymer Fracture", Vol 1, edited by E. H. Andrews (Applied Science Publishers, London, 1979).
14. N. VERHEUPEN-HEYMANS and J. C. BAUWENS, *J. Mater. Sci.* **11** (1976) 7.
15. S. TOLANSKY, "Multiple-beam Interferometry of Surfaces and Films", (Clarendon Press, Oxford, 1948).
16. L. E. NIELSON, "Mechanical Properties of Polymers", (Reinhold, New York, 1962) p. 131.
17. P. BEAHAN, M. BEVIS and D. HULL, *Proc. Roy. Soc.* **A343** (1975) 525.

Received 12 July 1979 and accepted 30 June 1980.